Order-Disorder Component in the Phase Transition Mechanism of ^{18}O Enriched Strontium Titanate

Robert Blinc,[1] Boštjan Zalar,[1] Valentin V. Laguta,[2] and Mitsuru Itoh[3]
[1]*Jožef Stefan Institute, Jamova 39, 1000 Ljubljana, Slovenia*
[2]*Institute for Problems of Material Sciences, Ukrainian Academy of Sciences, Krjijanovskogo 3, 03142 Kiev, Ukraine*
[3]*Materials and Structures Laboratory, Tokyo Institute of Technology, 4259 Nagatsuta, Midori, Yokohama, 226-8503, Japan*
(Received 27 August 2004; published 13 April 2005)

Ti and Sr nuclear magnetic resonance spectra of ^{18}O enriched $SrTiO_3$ (STO-18) provide direct evidence for Ti disorder already in the cubic phase and show that the ferroelectric transition at $T_C = 24$ K occurs in two steps. Below 70 K rhombohedral polar clusters are formed in the tetragonal matrix. These clusters subsequently grow in concentration, freeze out, and percolate, leading to an inhomogeneous ferroelectric state below T_C. This shows that the elusive ferroelectric transition in STO-18 is indeed connected with local symmetry lowering and implies the existence of an order-disorder component in addition to the displacive soft mode one. Rhombohedral clusters, Ti disorder, and a two-component state are found in the so-called quantum paraelectric state of STO-16 as well. The concentration of the rhombohedral clusters is, however, not high enough to allow for percolation.

DOI: 10.1103/PhysRevLett.94.147601 PACS numbers: 77.84.Dy, 76.30.Fc, 76.60.-k, 77.80.Bh

$SrTiO_3$ (abbreviated as STO-16) is considered [1] to be a classical displacive soft mode system where the ferroelectric phase is suppressed by zero point fluctuations of the soft mode leading to quantum paraelectricity [2]. The discovery of Itoh *et al.* [3] of a dielectric peak near $T_C \approx 24$ K in a 93% ^{18}O-isotope-exchanged $SrTiO_3$ (STO-18) sample seems to support this assumption [2], as the larger mass of ^{18}O reduces quantum zero point fluctuations and allows for the condensation of the polar soft mode at a nonzero T_C. The peak in the static dielectric constant appears as the concentration of the ^{18}O ions exceeds the critical concentration $x_c = 33\%$ and shifts to higher temperatures with increasing x. The appearance of a polarization hysteresis loop below T_C indicates that the dielectric peak indeed corresponds to the evolution of a ferroelectric state in STO-18.

Recent microscopic observations by inelastic neutron scattering [4] have, however, shown significant discrepancies with the above picture. The transverse optic E_U soft mode in STO-18 softens [5] but does not condense [4] at T_C. It is practically independent of the concentration of ^{18}O within the resolution of the neutron scattering experiment and the same as in STO-16 [4]. This indicates that the softening of the polar TO soft mode—though present [6]—is not the only mechanism driving the ferroelectric transition in STO-18 as assumed so far and that some other mechanism should be present, too.

Here we show that the low temperature state of STO-18 and STO-16 is below 70 K, in fact, a two-component one, and that polar rhombohedral clusters are embedded into a nonpolar tetragonal matrix. In STO-18 the clusters grow in intensity and percolate, leading to the formation of an inhomogeneous ferroelectric state below T_C. Similar clusters are seen in STO-16 as well, but their population is too small to allow for percolation. We have as well observed inherent Ti disorder in STO-18 and STO-16 already in the cubic phase coexisting with soft mode-type unit cell distortions [7]. The observation of first order quadrupole satellites in the Ti NMR spectra of both STO-16 and STO-18 demonstrates the presence of nonzero quadrupole coupling at the Ti sites. This is incompatible with the central position of the Ti ion in the oxygen octahedron and requires the presence of off-center Ti sites and Ti disorder. The angular dependence of the second moment of the satellite background in addition shows that on the NMR time scale the local structure of the macroscopically cubic phase consists of a random array of differently oriented soft mode-distorted tetragonal nanodomains in analogy to cubic $BaTiO_3$ [7–9]. The multivalley Ti potential surface does not seem to change with temperature.

The $^{87}Sr(I = 9/2)$, $^{47}Ti(I = 5/2)$, and $^{49}Ti(I = 7/2)$ NMR spectra have been measured in a magnetic field $B = 9.2$ T corresponding to Larmor frequencies of 16.471 and 21.406 MHz for the ^{87}Sr and $^{47,49}Ti$ isotopes, respectively. Because of a slight difference in their gyromagnetic moments, the Larmor frequencies of the ^{47}Ti and ^{49}Ti isotopes differ by 5.7 kHz in the field of 9.2 T giving rise to two sharp $1/2 \leftrightarrow -1/2$ central lines in the cubic phase. The measurements were performed on STO-18 single crystal samples (about 93% ^{18}O) [3] cut with two edges parallel to the (110) planes. The size of the STO-18 sample plates was $7 \times 3 \times 0.3$ mm^3. To increase the signal-to-noise ratio, 6–7 plates of STO-18 were attached together. The STO-16 measurements were performed on a $7 \times 4 \times 4$ mm^3 sample with the surfaces parallel to the (001) planes. The exorcycle pulse sequence has been used to observe the satellites [7].

The $^{47,49}Ti$ NMR spectra of STO-18 in the cubic phase at $T = 200$ K are shown in Fig. 1(a). We see in addition to the two sharp $1/2 \leftrightarrow -1/2$ central lines also a broad background due to unresolved $\pm 1/2 \leftrightarrow \pm 3/2$, $\pm 3/2 \leftrightarrow \pm 5/2, \ldots$ first order quadrupole coupling induced satel-

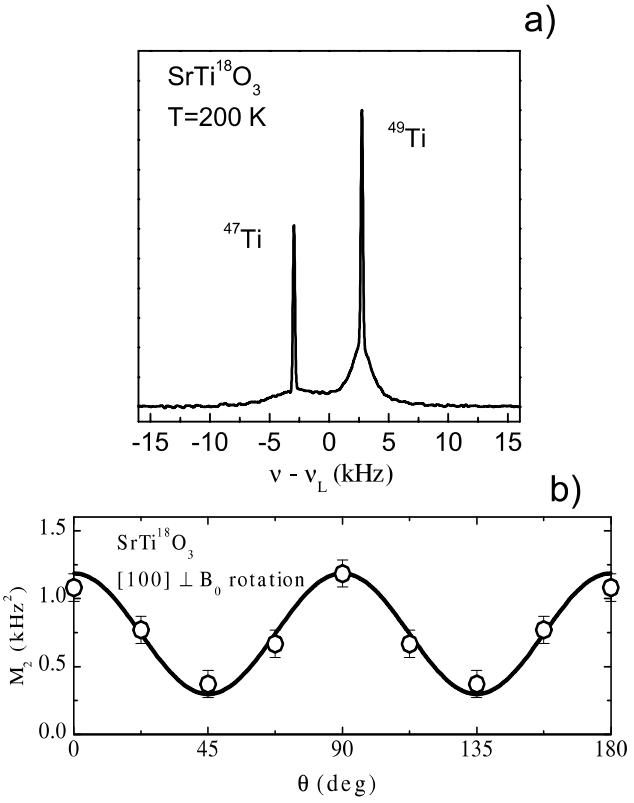

FIG. 1. (a) ^{47,49}Ti NMR spectra of $SrTi^{18}O_3$ in the paraelectric cubic phase. Note the broad unresolved satellite background in the Ti spectra demonstrating the breaking of the cubic symmetry and the sharp $1/2 \leftrightarrow -1/2$ central transition on top of it. (b) Angular dependence of the second moment of the satellite background of the ^{47}Ti spectra of STO-18 at $T = 200$ K. The solid line is the theoretical fit [7] for tetragonal distortions.

lites. The integral intensities of the two central lines and the broad background components are in the ratio $9/26 = 0.35$ and $4/17 = 0.24$, respectively, for the two Ti isotopes. This agrees with the predicted theoretical ratios for the intensities of the central components and the satellites in the ^{47}Ti and ^{49}Ti spectra [7], thus supporting the above assignment. Additional support comes from the fact that the width of the ^{47}Ti background component is about 2.5 times as large as the width of the ^{49}Ti component, in agreement with the ratio of their quadrupole frequencies ν_Q. The existence of satellites demonstrates the presence of a nonzero electric field gradient (EFG) tensor at the Ti sites and thus the local breaking of the cubic O_h symmetry by off-center displacements of the Ti ions.

In Fig. 1(b) we show the angular dependence of the second moment $M_2(\vartheta)$ of the satellite background of the ^{47}Ti spectra of STO-18 at 200 K. The best fit (solid line) shows that the local breaking of the cubic symmetry is tetragonal in analogy to cubic $BaTiO_3$ [7]. Within the 8-site Chavez model [8,9] developed for barium titanate, this means that the Ti ions are dynamically disordered between off-center sites displaced along the body diagonals and that four out of the eight off-center Ti sites are preferentially occupied. The $M_2(\vartheta)$ data also show [7] that on the NMR time scale the local structure of the cubic phase consists of a random array of six differently oriented polar tetragonal nanodomains. A similar $M_2(\vartheta)$ plot of the broad background component is obtained for STO-16.

The motionally averaged ^{47}Ti quadrupole frequency obtained from the M_2 data of STO-18 is at $T = 200$ K, $\nu_Q = 0.85$ kHz. This is significantly less than observed in the cubic phase of barium titanate [7] and shows that the lattice packing in STO is much tighter and the off-center sites are therefore closer to the center.

In contrast to the ^{47,49}Ti data, there is no such angularly dependent broad background component in the ^{87}Sr NMR spectra in the cubic phase. The Sr ion thus seems to occupy the high symmetry perovskite site in the cubic phases of both STO-18 and STO-16. In view of its position in the STO lattice, the EFG tensor at the ^{87}Sr site is much more sensitive to small distortions or rotations of the oxygen octahedra than the EFG tensor at the Ti site. This is important, as the eigenvector of the polar Slater mode in STO-18 should involve oxygen displacements as well as an effective shift of the Ti ion.

The temperature dependence of the shift of the central $1/2 \leftrightarrow -1/2$ Sr NMR transition at $\mathbf{B} \parallel [110]$ is shown in Fig. 2. At the cubic-tetragonal antiferrodistortive transition at $T_A = 104$ K, where alternations in the rotation directions of the oxygen octahedra in adjacent unit cells occur, the central ^{87}Sr NMR line splits into two components at this orientation. This is due to the presence of two nonequivalent tetragonal domains and the fact that the largest

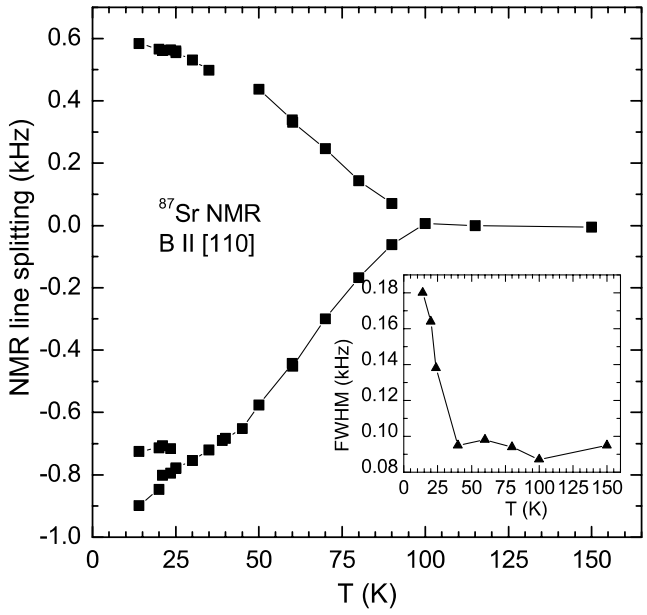

FIG. 2. Temperature dependence of the ^{87}Sr $1/2 \leftrightarrow -1/2$ central transition in STO-18 showing a line splitting at the cubic-tetragonal transition at $T_A = 104$ K. The insert shows the huge broadening of NMR line at $T_C = 24$ K in 95% ^{18}O enriched STO-18 which is absent in STO-16.

principal axis of the cylindrically symmetric Sr electric field gradient (EFG) tensor is parallel to the tetragonal axis of a given domain. The rotational order parameter extracted from the Sr NMR data agrees rather well with the one obtained from the EPR data of Müller *et al.* [10]. There is no such splitting in the Ti spectra.

The ^{87}Sr $1/2 \leftrightarrow -1/2$ spectra at $\mathbf{B} \parallel [111]$, where the ^{87}Sr NMR central lines of all tetragonal domains coincide, are shown in Fig. 3(a) at the different temperatures. There is a single Sr line between 100 and 70 K as expected on the basis of the tetragonal symmetry. Below 70 K the central Sr NMR line of STO-18 splits, demonstrating the existence of a two-component state. The more intense component still exhibits tetragonal symmetry whereas the second component which now consists of three narrow lines and a broad background [Fig. 3(b)] exhibits rhombohedral symmetry and shows in contrast to the tetragonal one a nonzero asymmetry parameter of the EFG tensor, $\eta = (V_{XX} - V_{YY})/V_{ZZ} = 0.08$. The temperature and angular dependence of this second component is different from that of the first component. The coexistence of the second component with the first one demonstrates the formation of rhombohedral clusters in the tetragonal matrix. The intensity of these clusters increases with decreasing temperature as shown in Fig. 4. It changes from zero to about 15% around 70 K, stays constant between 60 and 30 K, and reaches 60% at T_C. For the orientation $\mathbf{B} \parallel [110]$, the ferroelectric transition is accompanied by a huge increase in the ^{87}Sr NMR linewidth (insert to Fig. 2), indicating the onset of a multidomain state. A similar but much weaker rhombohedral ^{87}Sr NMR line appears also in STO-16 below 70 K. Since there is no such broadening or splitting of the NMR spectra as seen in STO-18, the concentration of these clusters seems here to be too low ($\sim 5\%$–6%) to allow for percolation.

The simulated and experimental rhombohedral Sr NMR spectra of STO-18 are compared in Fig. 3(b) for $\mathbf{B} \parallel [111]$ and $T = 16$ K, i.e., below T_C. The EFG tensor can be here described as a sum of two terms

$$\mathbf{V} = \mathbf{V}_0 + \begin{pmatrix} 0 & \tilde{V} & \tilde{V} \\ \tilde{V} & 0 & \tilde{V} \\ \tilde{V} & \tilde{V} & 0 \end{pmatrix}, \quad (1)$$

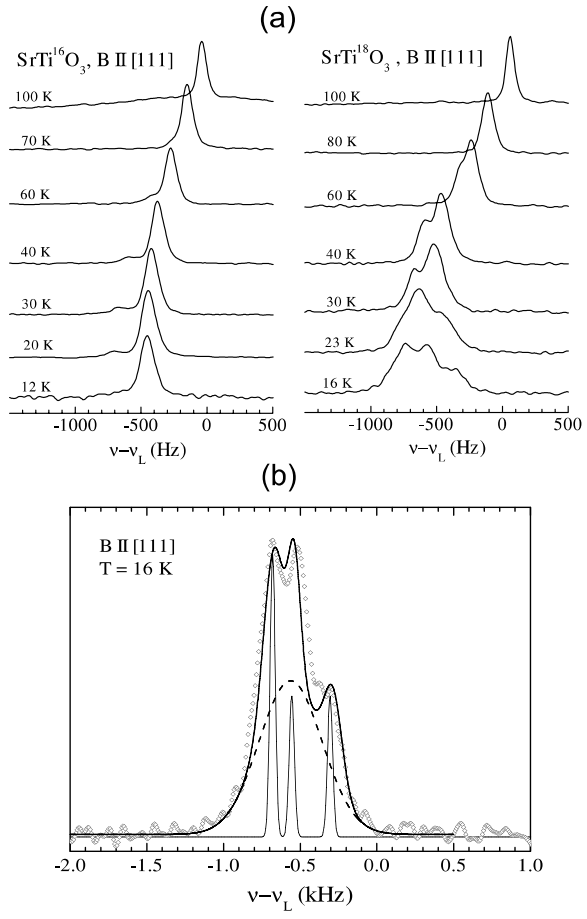

FIG. 3. (a) Comparison of the ^{87}Sr $1/2 \leftrightarrow -1/2$ NMR spectra of STO-16 and 95% ^{18}O enriched STO-18 above and below $T_C = 24$ K. (b) Simulated (solid lines) and measured (points) ^{87}Sr NMR $1/2 \leftrightarrow -1/2$ line shapes in STO-18 at $T = 16$ K $< T_C$ and $\mathbf{B} \parallel [111]$.

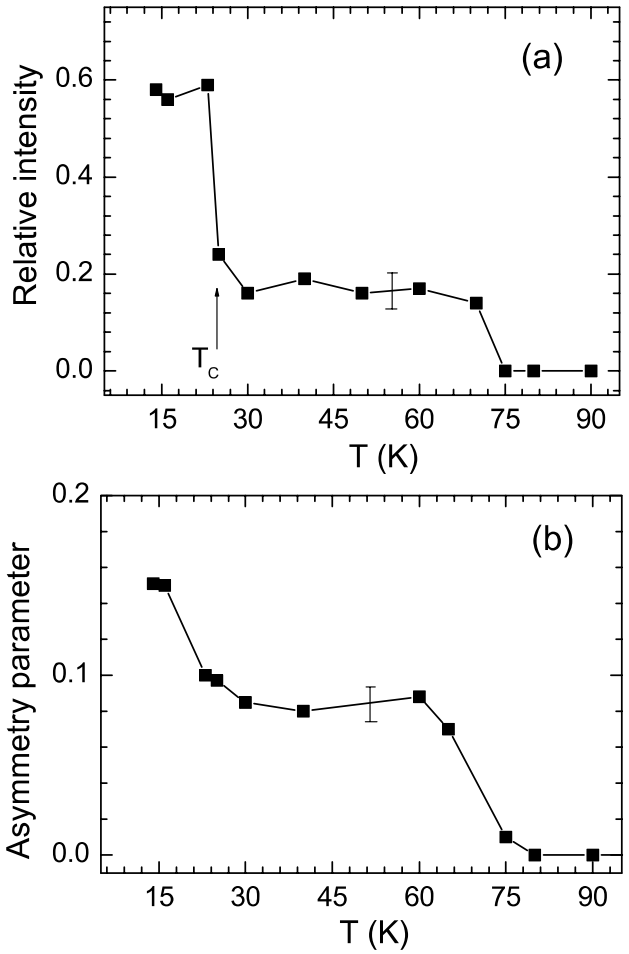

FIG. 4. Temperature dependence of the relative intensity (a) and the ^{87}Sr asymmetry parameter η (b) of the rhombohedral clusters in STO-18.

where $\mathbf{V}_0$ is the EFG tensor of the tetragonal STO lattice below $T_A = 104$ K and the second term represents a small ($\sim V_{ZZ}/10$) rhombohedral $\langle 111 \rangle$-type perturbation. Distortions of any other symmetry will also produce diagonal components resulting in a large splitting of the spectrum at $\mathbf{B} \parallel [110]$ which has not been observed. The EFG tensor of the rhombohedral clusters which appear below 70 K can be as well described by expression (1).

The rhombohedral EFG tensor has two principal axes slightly (5°) tilted from the $\langle 001 \rangle$ and $\langle 110 \rangle$ cubic directions. The deviation from cylindrical symmetry is significant and the asymmetry parameter is $\eta \approx 0.16$. The corresponding EFG tensor eigenvalues are: $V_{ZZ} = -3.35 \times 10^{20}$ V/m^2, $V_{YY} = 1.98 \times 10^{20}$ V/m^2, and $V_{XX} = 1.41 \times 10^{20}$ V/m^2. The **x**, **y**, **z** principal axes have the following polar (ϑ) and azimuthal (φ) angles for the [001] domain: $\mathbf{x} \rightarrow (90°, 315°)$, $\mathbf{y} \rightarrow (85°, 45°)$, and $\mathbf{z} \rightarrow (5°, 225°)$.

Point charge calculations show that such a rhombohedral perturbation can reflect O^{2-} shifts along the $\langle 111 \rangle$ directions of the order of 0.02 Å (or equivalently O^{2-}-Sr bond distance changes of this magnitude). The superposition of the rhombohedral distortions on the tetragonally deformed lattice will result in a triclinic symmetry of the low temperature phase.

The temperature dependence of the asymmetry parameter η of the rhombohedral EFG tensor **V** is shown in Fig. 4. It changes from zero to about 0.08 around 70 K and shows a significant increase to 0.16 at T_C. The ^{87}Sr quadrupole frequency ν_Q varies between zero at $T_A = 104$ K and $\nu_Q = 70$ kHz at T_C. A change is seen here, too, both at 70 K and at T_C, but the effect of the phase transition on the quadrupole frequency is much smaller than in the case of the asymmetry parameter.

The ^{47,49}Ti spectrum varies little with temperature and shows no splitting of the central lines either at the antiferro distortive transition at $T_A = 104$ K nor at the ferroelectric transition at $T_C = 24$ K. This is in contrast to the case of barium titanate where the central line splits [7] due to 90° domains at the cubic-tetragonal transition. There is, however, a shift of the central Ti NMR line in STO-18 on cooling from 30 to 15 K at $\mathbf{B} \parallel [111]$ whereas there is no such shift in STO-16.

The broad Ti satellite background starts to disappear at lower temperatures and is transformed into resolved satellite peaks already at about 70 K, i.e., in the temperature range where rhombohedral clusters can be detected in the Sr NMR spectra. Around $T = 24$ K, the Ti quadrupole frequency increases to 15 kHz, indicating Ti ordering. This is in agreement with the observed increase in the Ti spin-lattice relaxation time.

The obtained results show the existence of a two-component state in both STO-16 and STO-18 at low temperatures. Below 70 K, polar rhombohedral clusters are embedded in a nonpolar tetragonal matrix. In STO-18 the clusters grow in intensity and percolate as T approaches T_C, leading to an inhomogeneous ferroelectric state. In STO-16 their population is too small to allow for percolation. The difference between STO-18 and STO-16 may be due to the fact that the intercluster interaction constant [11,12], which depends on the inverse square of the soft phonon frequency, is larger than a critical value in STO-18 and smaller than that in STO-16. Our results also demonstrate that Ti disorder is present already in the cubic phases of STO-18 and STO-16. The results demonstrate the presence of an order-disorder component in the ferroelectric phase transition mechanism of STO-18 in addition to the soft mode one. The discovery of the presence of disorder in STO thus validates the early ideas Slater and Müller of the "rattling" Ti ion [13] as being at the heart of the structural phase transition mechanism in perovskites.

[1] W. Cochran, Adv. Phys. **9**, 387 (1960). See also J. F. Scott, Rev. Mod. Phys. **46**, 83 (1974).

[2] K. A. Müller and H. Burkhard, Phys. Rev. B **19**, 3593 (1979); see also T. Hidako, Ferroelectrics **137**, 291 (1992); W. Zhong and D. Vanderbilt, Phys. Rev. B **53**, 5047 (1996); M. Maglione, R. Bohmer, A. Loidl, and U. T. Hochli, Phys. Rev. B **40**, 11441 (1989).

[3] M. Itoh, R. Wang, Y. Inaguma, T. Yamaguchi, Y.-J. Shan, and T. Nakamura, Phys. Rev. Lett. **82**, 3540 (1999).

[4] Y. Noda (private communication); Y. Yamada, N. Todoroki, and S. Miyashita, Phys. Rev. B **69**, 024103 (2004).

[5] Y. Minaki, M. Kobayashi, Y. Tsujimi, T. Yagi, M. Nakanishi, R. Wang, and M. Itoh, J. Korean Phys. Soc. Suppl. **42**, S11290 (2003).

[6] E. I. Venturini, G. A. Samara, M. Itoh, and R. Wang, Phys. Rev. B **69**, 184105 (2004); N. Sai and D. Vanderbilt, Phys. Rev. B **62**, 13942 (2000).

[7] B. Zalar, V. V. Laguta, and R. Blinc, Phys. Rev. Lett. **90**, 037601 (2003); B. Zalar, A. Lebar, I. Seliger, R. Blinc, V. V. Laguta, and M. Itoh, Phys. Rev. B **71**, 064107 (2005); see also T. J. Bastow, J. Phys. Condens. Matter **1**, 4985 (1989); O. Kanert, H. Schulz, and J. Albers, Solid State Commun. **91**, 465 (1994).

[8] A. S. Chaves, F. C. S. Barreto, R. A. Nouqueira, and B. Žekš, Phys. Rev. B **13**, 207 (1976).

[9] E. A. Stern, Phys. Rev. Lett. **93**, 037601 (2004).

[10] K. A. Müller and W. Berlinger, Phys. Rev. B **34**, 6130 (1986).

[11] R. Blinc, V. Laguta, and B. Zalar, Phys. Rev. Lett. **91**, 247601 (2003).

[12] R. Blinc, V. Bobnar, and R. Pirc, Phys. Rev. B **64**, 132103 (2001).

[13] See, for instance, K. A. Müller, W. Berlinger, and K. W. Blazey, Solid State Commun. 61, 21 (1987); J. C. Slater, Phys. Rev. **78**, 748 (1950); MIT Seminar, 1960 (unpublished); B. Matthias and A. von Hippel, Phys. Rev. **73**, 1378 (1948).